Jestr

Journal of Engineering Science and Technology Review 15 (SI) (2022) 8 - 15
Special Issue in honor of Prof. T. Tanaka

JOURNAL OF
Engineering Science and Technology Review

www.jestr.org

Research Article

A Trial to Estimate the Content and Distribution of Filler in Polymer Nanocomposites by SEM-EDX

Yoshimichi Ohki* and Naoshi Hirai

Research Institute for Materials Science and Technology, Waseda University,2-8-26 Nishiwaseda, Shinjuku-ku, Tokyo 169-0051, Japan

Received 15 December 2021; Accepted 26 February 2022

Abstract

Reflecting the fact that this paper is to be included in a special issue to celebrate the 83rd birthday of Prof. T. Tanaka, a brief introduction of the scientific mutual relationship between the corresponding author of the present paper and Tanaka is mentioned. Then, reflecting the prime importance to estimate the entire content and spatial distribution of filler in polymer nanocomposites, a trial to convert two-dimensionally measured values of filler content to three-dimensional values is developed. Next, it is demonstrated that energy-dispersive X-ray (EDX) analysis using scanning electron microscopy (SEM) can be a reliable and industrially feasible tool to estimate the filler content. Furthermore, by conducting the SEM-EDX analyses under different magnifications and by analyzing the magnification-dependence of the filler content, the spatial dispersity of the filler in the nanocomposite can be evaluated.

Keywords: insulating polymer, machine insulation, additive content, filler distribution, filler dispersity

1 Introduction

1.1 Scientific Relationship with Prof. T. Tanaka

The date the corresponding author (YO) of the present paper first met Dr. T. Tanaka is 18 September 1972. That day was the first day of the Fifth Symposium on Electrical Insulating Materials (SEIM), which was held at the Zendentsu Hall, Kanda, Tokyo, Japan. Although the detailed history of this symposium can be found elsewhere [1], this symposium was, in short, inaugurated in 1968 as a Japanese version of the Conference on Electrical Insulation, annually held in the USA. Dr. T. Tanaka was an assistant secretary of the Fifth SEIM, and YO was a senior undergraduate student in the Yahagi Laboratory, Waseda University, and dispatched from the laboratory to help the symposium as a student worker. YO already knew Tanaka at that time through reading many of his research papers in the field of electrical insulation since the theme of YO's graduation thesis was electro-luminescence in polyethylene and its relation to electrical treeing. By that time, YO acquired a strong impression that Tanaka would be a key person in the research on electrical insulating materials since all his papers were full of scientific insights.

Since they first met, YO continued to keep in contact with Dr. Tanaka. Many things that YO did or has been conducting until today are the succession of what Tanaka had done. The contribution of articles to the News from Japan column in the Electrical Insulation Magazine issued by the Dielectrics and Electrical Insulation Society, IEEE, is one such example. For 16 years from 1972 to 1987, Dr. Tanaka was a regular contributor to that column [1]. Since the succession of Tanaka's role, YO has been continuing to send articles to the column without lacking any issue for 34 years. Through this work, YO has understood the statuses quo of Japanese research and development (R&D) activities in industry and academia. Some of such R&D activities in Japan reviewed by YO, concerning polymer nanocomposites, will be introduced in the next section of this paper.

The next important occasion between Dr. Tanaka and YO occurred around 2000. Around those years, Waseda University, where YO has been working since his graduation, planned to open a new graduate school, Graduate School of Information, Production and Systems (IPS) on a new campus in Kita-Kyushu. In this regard, YO was asked to find candidates of professors in the field of electrical engineering by the appointed new Dean of the graduate school. In responding to this request, YO immediately recommended Dr. Tanaka, which was soon approved by the university's professor selection committee.

Before Dr. Tanaka became a full professor of Waseda University in April 2002, he had been an adjunct professor at the university, affiliated with the YO's laboratory, from October 2001 to March 2002. Since then, Prof. Tanaka and YO operated the Tanaka-Ohki laboratory cooperatively until the Graduate School of IPS opened in April 2003. Dr. Masahiro Kozako, now an associate professor at Kyushu Institute of Technology, began working in April 2002 as a research associate in the Tanaka-Ohki laboratory.

Around those days, polymer nanocomposites (PNCs) appeared and were recognized as an emerging innovative electrical insulating material. Regarding this, Prof. Tanaka and Dr. Kozako as well as YO decided on PNCs as a research topic to examine in their laboratory. Since then, Prof. Tanaka conducted much research on PNCs in several research groups in the Tanaka-Ohki laboratory and his laboratories in IPS and later in the Xi'an Jiaotong University, China. The splendid R&D achievements conducted mostly on PNCs by those groups headed by Prof. Tanaka have been well known worldwide.

*E-mail address: yohko@waseda.japan
ISSN: 1791-2377 © 2022 School of Science, IHU. All rights reserved.
doi:10.25103/jestr.147.02

1.2 Estimation of the Content and Distribution of Filler

Polymer NCs, in which inorganic fillers with a size of approximately 1 μm or less are dispersed in polymers, are attracting much attention as they exhibit excellent electrical insulation performance and mechanical properties [2-9]. If someone inquires the authors to show three issues related to filler when producing PNCs, their answer would be the reduction in content of filler in the sample due to its adhesion to the production equipment, its uneven distribution in the sample, and its aggregation. Of these three items, the aggregation of filler seems to attract attention, as shown by the fact that to show scanning electron microscopy (SEM) images of samples is semi-standardized for the submission of papers on PNCs. The non-uniform distribution of filler also attracts attention in relation to the aggregation of filler. Compared to these, the authors have the impression that the decrease in the content of filler added to the sample has not attracted as much attention as its importance.

There are many quantitative analysis methods of elements in solids, such as chemical analysis, inductively coupled plasma mass spectrometry, Auger electron spectroscopy, and X-ray fluorescence spectroscopy, if we include destructive methods. In this study, we attempt to evaluate the reduction in the filler content due to adhesion to the production equipment and the uneven filler distribution in the sample, by performing frequently used energy-dispersive X-ray (EDX) analysis using SEM.

2. Industrial applications of PNCs

Several PNCs are already used in the industry as electrical insulating materials. Examples of applications of PNCs realized industrially in several pieces of power apparatus, mainly focusing on those in Japan, are reviewed in the books edited by Prof. T. Tanaka [10,11]. The corresponding author of the present paper also introduced several applications of PNCs in the News from Japan column [12-17], which was succeeded after Prof. Tanaka, as mentioned above. The application of PNCs to electrical insulation in Japan was first realized in magnet wires for coil windings in rotating electric machines [12]. Then, it followed as the world-first polymeric insulation in DC power cables [13-16]. In addition, using nano-microcomposite reported in [17] for electrical insulation, solid-state switchgear was developed and has already been installed widely in the world [18].

Concerning the application of PNCs as electrical insulating materials for magnet wires in rotating electric machines, a big R&D project, funded by a public organization called New Energy and Industrial Technology Development Organization (NEDO), is currently underway in Japan. This project has a preceding NEDO project. The two projects were started by the strong initiative of Prof. Tanaka, and YO was the head researcher of the previous project and is one of the principal researchers of the ongoing one.

The currently ongoing project consists of three sub-projects. Among them, two sub-projects have the common objective to reduce the thickness of insulating materials of the coil windings in power generators. One sub-project aims at developing the PNC insulation for power generators up to the 1.5-kVA class using polyimide as the host resin [19-21], while the other sub-project for larger generators has been searching for the best PNC that can match the host epoxy resin [22–27]. The target of the other sub-project is to develop innovative functionally graded electrical insulation suitable for spacers in gas-insulated switchgear through the well-designed distribution of proper micro-sized and nano-sized inorganic fillers with different values of permittivity in epoxy resin [28,29].

3. Samples and experimental procedures

The present research is related to the above NEDO sub-project for power generators up to the 1.5-kVA class. The samples used are polyimide NCs with boehmite alumina added as a filler. Tab. 1 lists their names, substance of filler, filler content, approximate filler size, and treatment method of filler surface.

Table 1. Samples

Sample	Filler	Filler Content (wt%)	Particle Size (nm)	Surface treatment
A10	AlOOH	10	10×50	NA[1]
A20	AlOOH	20	10×50	NA[1]
AM10	AlOOH	10	20	MSCA[2]
AE10	AlOOH	10	10×50	ESCA[3]
AE20	AlOOH	20	10×50	ESCA[3]

1: Not applicable, 2: Surface treated with methacrylic silane coupling agent, 3: Surface treated with epoxy silane coupling agent.

Since the objective of the present research is to develop the insulation of coil windings for power generators, the sample thickness is about 50 to 100 μm. The letter A in the sample name stands for polyimide NCs in the case when the boehmite alumina filler was not surface-treated, while the samples are called AM and AE when the filler surface was treated with a methacrylic silane coupling agent and an epoxy-based silane coupling agent, respectively. Next to the letters A, AM, and AE, the filler content in wt% was added as in the case of A10. The polyimide used in this study is a kind of copolymer of Kapton and UPILEX [19, 21]. The details of the samples, including the base polyimide, filler, manufacturing process, and surface treatment method, were already reported elsewhere [21].

The surface of each sample was observed by field-emission SEM (IT-100LA, JEOL) with an acceleration energy of 3 kV, while EDX spectral mapping was conducted with an EDX spectrometer (JED-2300, JEOL). For these measurements, the sample surface or cross-section was smoothened by the broad ion beam (BIB) polishing using Ar ions and coated with Pt. As the elements to detect by EDX, C, O, Al, and Si were selected.

4. Theory

4.1. Estimation of the filler content

4.1.1. Data Conversion from 2D to 3D

Part 1: Equations for the Conversion Developed Based on Crystal Forms

Images observed by SEM or SEM-EDX are two-dimensional (2D). Therefore, to know the filler content in the PNC sample, we have to convert 2D data to three-dimensional (3D) values. Here, we are going to find the relationship between the 3D filler content (vol%) R_3 and the 2D area occupancy of fillers (area%) R_2 measured by SEM or SEM-EDX. Here, we consider the atomic packing factor of a crystal, namely the maximum filling factor of the crystal containing many atoms of only one type so that they do not overlap. In order to relate to the filler content in a PNC, the volume of the crystal structure is regarded as that of the sample, and the atom is regarded as the filler so that the atomic packing factor of the crystal corresponds to the 3D filler content (vol%) in the PNC.

(1) Simple cubic crystal: In a simple cubic crystal consisting of many identical atoms with the side length a, the maximum atom radius r is given by the equation,

$$r = a/2 \quad (1)$$

From this, the atomic packing factor of simple cubic crystals or the corresponding maximum filler content (vol%) becomes

$$R_3 = \frac{\frac{4}{3}\pi\left(\frac{a}{2}\right)^3}{a^3} = \pi/6 = 0.524 = 52.4 \text{ (vol\%)} \quad (2)$$

At this time, the area occupancy R_2 of the atoms becomes the maximum on a {100} lattice plane of the simple cubic lattice and is given by

$$R_2 = \frac{\pi r^2}{a^2} = \frac{\pi}{4} = 0.785 \quad (3)$$

On the other hand, since atoms do not intersect {200} lattice planes,

$$R_2 = 0 \quad (4)$$

at these planes. Therefore, R_2 varies from the minimum of 0 to the maximum of 0.785 in a simple cubic crystal. Here, if we calculate their average R_{2Av},

$$R_{2Av} = \pi/8 = 0.393 = 39.3 \text{ (area\%)} \quad (5)$$

Therefore, assuming simple cubic crystals, a sample with the 3D filler content of 52.4 (vol%) would be measured to have the apparent 2D content of 39.3 (area%) in SEM images. The ratio of R_{2Av} to R_3 is

$$R_{23} = R_{2Av}/R_3 = 3/4 = 0.75 \quad (6)$$

(2) Face-centered cubic crystal: In a face-centered cubic crystal consisting of many identical atoms with the side length a, the maximum atom radius r is given by the equation,

$$r = \sqrt{2}a/4 \quad (7)$$

In this regard, the corresponding maximum filler content becomes

$$R_3 = 4 \times \frac{\frac{4}{3}\pi\left(\sqrt{2}a/4\right)^3}{a^3} = \frac{\sqrt{2}\pi}{6} = 0.740 = 74.0 \text{ (vol\%)} \quad (8)$$

On the other hand, R_2 on the {100} planes of the face-centered cubic lattice is

$$R_2 = 2 \times \frac{\pi r^2}{a^2} = \frac{\pi}{4} = 0.785 \quad (9)$$

In addition, R_2 is also calculated on the {200} planes as

$$R_2 = 2 \times \frac{\pi r^2}{a^2} = \frac{\pi}{4} = 0.785 \quad (10)$$

Their average R_{2Av} is

$$R_{2Av} = \pi/4 = 0.785 = 78.5 \text{ (area\%)} \quad (11)$$

Consequently, assuming a face-centered cubic crystal, a sample with the 3D filler content of 74.0 (vol%) would be measured to have the apparent 2D content of 78.5 (area%) in SEM images. The ratio of R_{2Av} to R_3 is

$$R_{23} = R_{2Av}/R_3 = 3/(2\sqrt{2}) = 1.061 \quad (12)$$

(3) Body-centered cubic crystal: By doing similar calculations, we obtain

$$r = \sqrt{3}a/4 \quad (13)$$

$$R_3 = 2 \times \frac{\frac{4}{3}\pi\left(\sqrt{3}a/4\right)^3}{a^3} = \frac{\sqrt{3}\pi}{8} = 0.680 = 68.0 \text{ (vol\%)} \quad (14)$$

While R_2 becomes

$$R_2 = \frac{\pi r^2}{a^2} = \frac{\pi(\sqrt{3}a/4)^2}{a^2} = \frac{3\pi}{16} = 0.589 \quad (15)$$

on the {100} planes, it also becomes

$$R_2 = \frac{\pi r^2}{a^2} = \frac{3\pi}{16} = 0.589 \quad (16)$$

on the {200} planes. In addition, it is calculated to be

$$R_2 = 2\frac{\pi r^2}{\sqrt{2}a^2} = 2\frac{\pi(\sqrt{3}a/4)^2}{\sqrt{2}a^2} = \frac{3\sqrt{2}\pi}{16} = 0.833 \quad (17)$$

on the {110} planes. Therefore, we obtain

$$R_{2Av} = 0.670 = 67.0 \text{ (area\%)} \quad (18)$$

And

$$R_{23} = R_{2Av}/R_3 = 0.985 \quad (19)$$

Although R_2 could be calculated for each sliced cross-section to obtain a more accurate R_{23} if we use a computer, the average of the values mentioned in (6), (12), and (19) becomes

$$R_{23} = R_{2Av}/R_3 = 0.932 \quad (20)$$

Consequently, in order to convert the area occupancy R_2 in area% of the filler acquired by 2D measurements such as SEM images into the 3D content R_3 in vol%, we can divide R_2 by the factor of 0.932. In other words, the 3D volume content R_3 is calculated to be higher than the 2D area occupancy R_2.

Part 2: Equations for the Conversion Developed Based on Particles in a Cube

Next, we assume a simple model that many identically small spherical particles are uniformly dispersed in a cube significantly larger than the particles. Let L and D be the side

length of the cube and the diameter of the particles, respectively. First, we think of a 1D situation. If n particles are put uniformly on the side with the length L of the cube, the highest value of the occupancy R_1 of the side by the particles becomes

$$R_1 = {nD}/{L} \tag{21}$$

Next, we think of one square plane of the cube with its side L as a 2D situation. Here we assume that n^2 particles should appear on the plane with the area L^2 if the number of the particles on one side with the length of L is n. Then, if n^2 particles are present uniformly on the plane with the area L^2, the highest value of the area occupancy R_2 of the plane by the particles becomes

$$R_2 = {n^2\pi D^2}/{4L^2} = \frac{\pi}{4}R_1^2 \tag{22}$$

Lastly, we think of the cube with its side L as a 3D situation. If we can assume a hypothesis similar to the above, n^3 particles should be in the cube with the volume L^3. Then, the highest value of the volume occupancy R_3 of the cube by the particles becomes

$$R_3 = {n^3 4\pi D^3}/{24L^3} = \frac{\pi}{6}R_1^3 \tag{23}$$

Therefore, when the 2D area% estimated from a SEM image is represented by R_2 and its 3D volume content in vol% in the sample is represented by R_3, the ratio R_{23} becomes

$$R_{23} = \frac{R_2}{R_3} = \frac{3}{2}R_1^{-1} \gg 1.0 \tag{24}$$

One point here is that R_1, R_2, and R_3 we assumed here are their respective maxima. Regarding this, if we can assume similar relations for other values of R_1, R_2, and R_3, it can be said that R_{23} would be not so high as defined by Eq. (24). Consequently, it has become clear that the 2D area occupancy R_2 would be measured higher than the 3D volume content R_3, but not so high as $(3/2)R_1^{-1} = 3L/(2nD)$.

Here, if we regard that $\pi / 4 \approx 1.0$ and $\pi / 6 \approx 1.0$, we have

$$R_2 \approx R_1^2 \tag{25}$$

and

$$R_3 \approx R_1^3 \tag{26}$$

from Eqs. (22) and (23), respectively. These equations demonstrate the validity of the approximation we will use in the next subsection 4.1.2.

Depending on whether we trust Eq. (20) in Part 1 or Eq. (24) in Part 2, R_{23} becomes either lower or higher than 1.0. Then, which is correct? One important thing is that the surface area and the volume of a sphere depend on its diameter D in the shapes of D^2 and D^3, respectively. Therefore, the volume or volume-related quantities, such as the mass, become smaller much faster than the surface area when D becomes smaller. Regarding this, the discussion developed in Part 1 based on the atomic packing factors of crystals seems out of the point since we assumed the largest possible atomic diameter. Since we are treating nanofiller, we regard that R_{23} is higher than 1.0. That is, the 2D area occupancy R_2 is measured higher than the 3D volume content R_3.

4.1.2. Estimation of the Filler Content by SEM-EDX

The estimation of the filler content from the ratio of the filler area to the total area of a SEM image is widely used. However, in SEM images, for example, the possibility that foreign objects such as voids, impurities, and dust on the sample surface are mistaken for fillers cannot be ignored. This risk can be avoided by identifying the element by SEM-EDX since the characteristic X-rays detected by EDX have unique energies peculiar to the element [30]. Therefore, let us consider a method for estimating the 2D area% and 3D weight% (wt%) of the filler from the atomic percentage of the element identified by SEM-EDX.

In the case of a composite of inorganic substances as well as the donor or acceptor concentration in semiconductors, it would not be difficult to calculate the wt% or volume% of each component from the atomic percentage of each element by considering the chemical formula and density of each component and the mass of each constituent element. However, making a similar estimation with PNCs is impossible precisely and rather difficult even approximately.

As mentioned above, the polyimide used in this study is a kind of copolymer of Kapton and UPILEX [19,21], but for the sake of simplicity, if we regard it as Kapton H, its repeating unit has a structure of $C_{22}O_5N_2H_{10}$ [31]. In the case of a polymer, since its molecular weight depends on the number of repeating units, we cannot use its value as it is. Therefore, we treat virtually this repeating unit as the polyimide we used. The molecular weight or the mass of 1 mol of the repeating unit is 382 g, in which 264 g of C, 80 g of O, 28 g of N, and 10 g of H are present.

On the other hand, the chemical formula of boehmite alumina is AlO(OH), and its molecular weight is 60 g, consisting of Al of 27 g, O of 32 g, and H of 1 g. From the above information, let us calculate the 3D mass percentage or wt% of Al that should be measured in sample A10 containing 10 wt% of boehmite alumina. If we have 1 mol of AM10 with the boehmite alumina content of 100δ mol%, according to the above definition, the condition that its content becomes 10 wt% is expressed as follows:

$$\frac{60\delta}{382(1-\delta)+60\delta} = 0.1 \tag{27}$$

From this, we obtain $\delta = 0.4143$. That is, we have to add boehmite alumina by 41.43 mol%. The story goes awry, but the number varies significantly, depending on whether the content is expressed in wt% or mol%. The remaining 58.57 mol% is the polyimide. In this regard, the masses or weights of C, O, and Al are (264 x 0.5857 =) 154.6 g for C, (80 x 0.5857 + 32 x 0.4143 =) 60.1 g for O, and (27 x 0.4143 =) 11.2 g for Al. In other words, the mass abundance ratio of C, O, and Al is C: O: Al = 154.6: 60.1: 11.2. Therefore, if we have AM10 according to the above definition of virtual polyimide, the apparent 2D abundance ratio of C, O, and Al in the observation area of SEM-EDX becomes C: O: Al = $(154.6)^{2/3}$: $(60.1)^{2/3}$: $(11.2)^{2/3}$ = 28.8: 15.4: 5.0 if we trust the discussion developed in Part 2 of 4.1.1.

Tab. 2 lists the mass ratios of the elements measured by SEM-EDX on a cross-section of AM10. Among the elements we calculated their masses, we measured the abundance of C and O as two representative elements of polyimide. In addition, Al and Si were chosen to represent boehmite alumina surface-treated by the silane coupling agent, although we would not use Si for the analyses.

Table 2. Mass ratios of elements (cross- section of AM10)

Element	Mass ratio (wt%)
C	62.2
O	29.8
Al	6.6
Si	1.4
Total	100.0

Paying attention that the total wt% of the three elements excluding Si is 98.6% in Tab. 2, the wt% of Al to be measured by SEM-EDX in AM10 is calculated as

$$[\mathrm{Al}] = \left(\frac{5.0}{28.8+15.4+5.0}\right) \times 0.986 = 0.100 \quad (28)$$

That is, the wt% to be measured for Al in sample AM10 should be 10.0 wt%. The corresponding mass ratio of Al listed in Tab. 2 is 6.6 wt%. Here, $(6.6/10.0)^{3/2}$ is 0.54.Therefore, if all the above calculations are correct, boehmite alumina remaining in sample AM10 is 54 % of the designed value.

Similarly to the above, we will calculate the 2D mass (= wt)% of Al that should be measured by SEM-EDX for sample AE20. First, as the condition that the content of boehmite alumina becomes 20 wt%, we have

$$\frac{60\delta}{382(1-\delta)+60\delta} = 0.2 \quad (29)$$

By solving the above, we obtain δ = 0.614. Then, the weights of C, O, and Al are calculated to be (264×0.386 =) 101.9 g for C, (80×0.386 + 32 × 0.614 =) 50.5 g for O, and (27 × 0.614 =) 16.6 g for Al. This means that the 3D mass abundance ratio of C, O, and Al is C : O : Al = 101.9 : 50.5 : 16.6. Therefore, under the same assumption, the apparent 2D mass abundance ratio of C, O, and Al becomes C : O : Al = $(101.9)^{2/3}$: $(50.5)^{2/3}$: $(16.6)^{2/3}$ = 21.8 : 13.7 : 6.5.

Tab. 3 lists the mass ratios of the elements measured by SEM-EDX on a cross-section of AE20. Since the total wt% of the three elements other than Si is 97.1% in Tab. 3, the wt% of Al to be measured by SEM-EDX in AE20 is calculated to be

$$[\mathrm{Al}] = \left(\frac{6.5}{21.8+13.7+6.5}\right) \times 0.971 = 0.150 \quad (30)$$

Therefore, the wt% to be measured for Al in sample AE20 should be 15.0 wt%. If we compare this value with the corresponding value of 8.8 wt% listed in Tab. 3, boehmite alumina remaining in sample AE20 is found to be 45 % of the designed value since $(8.8/15.0)^{3/2}$ is 0.45.

If the abundance ratios of the elements measured by SEM-EDX listed in Tab. 2 and 3 were correct even in 3D, it turns out that sample AE20 contains filler about (8.8/6.6=) 1.33 times as high as AM10, despite their designed ratio of 2.0 times. However, if we assume according to the discussion developed in Part 2 of 4.1.1 that the ratio in 3D volume% is the ratio in 2D area% to the power of (3/2), AE20 has $(1.33)^{3/2}$ = 1.54 times more filler than AM10.

Table 3. Mass ratios of elements (cross-section of AE20)

Element	Mass ratio (wt%)
C	57.3
O	31.0
Al	8.8
Si	2.9
Total	100.0

However, for such conversion between 2D and 3D, when we calculate the abundance ratio of each constituent atom, the sum of the abundance ratios of all the constituent atoms in 3D or 2D must be 1.0. Strictly speaking, this is impossible for PNCs since SEM-EDX cannot detect H. Furthermore, when we convert a 3D value to the corresponding 2D value using the approximation that the latter is the (2/3) power of the former, it would be good if we consider the atomic% of the constituent atoms. However, when considering the mass ratio, for example, even if we multiply the mass number 12 to the apparent 2D number of carbons calculated by the above conversion, we cannot find the apparent 2D mass of carbons. The reason for this is that the above conversion is also needed on the mass number of C.

The ratio between the mass percentages of Al to be measured in AM10 and AE20, shown respectively in Eqs. (28) and (30), is 1.50 and its (3/2) power is 1.84. Regarding this, this value of 1.84 does not match the assumed Al ratio in wt%, 2.0, between AM10 and AE20. This is probably because the presence of N contained in polyimide and Si contained in the surface treatment agent were not included in the conversion.

4.2. Estimation of the spatial distribution of filler

When we measure the atomic percentage or mass percentage of the element of the filler at a certain same place by SEM-EDX under different magnifications, we can examine the magnification dependence of the abundance of filler. The difference in observation magnification means the difference in the size of the surface to be observed. For example, suppose that there is an aggregation of filler that occupies most of the observation area of about 40 μm square of SEM-EDX mapping with a magnification of 3,000 times. If we observe this point, the atomic percentage of the filler element is naturally high. When the magnification is lowered without changing the center point, if many resin parts that are not fillers come into the observation area, the atomic percentage of the filler element will decrease.

On the other hand, when the atomic percentage of the filler element increases when the magnification is lowered, it is presumed that there is an aggregated filler outside the original observation area at the high magnification, which comes into the new observation area. That is, if we observe the same point with SEM-EDX under different magnifications and examine the observation magnification dependence of the abundance ratio of the filler elements obtained from it, we can estimate the spatial distribution of the filler. Of course, the correct 3D abundance ratio can be used for this purpose, but the use of the apparent 2D abundance ratio of the filler element is sufficient.

5. Results

Fig. 1 shows the SEM backscattered electron image taken under the magnification of 9,500 times and the EDX mapping of Al observed on a fracture surface or cross-section of sample AM10. Several egg-like objects in a range from 0.4 to 0.9 μm are seen in Fig. 1(a). They are silica, which appears as residues of the surface treatment, especially clearly on the surface of the samples surface-treated by the methacrylic silane coupling agent like this sample AM10 [21]. In Fig. 1(b), the color bars besides the EDX mapping represent the intensities of the characteristic X-rays that correspond to the abundance of Al atoms. Here, the lowest and highest intensities are represented by the black and the white bars, respectively, while the green and red ones show the intermediates. Despite the presence of the egg-like objects, Al appears to be present almost uniformly.

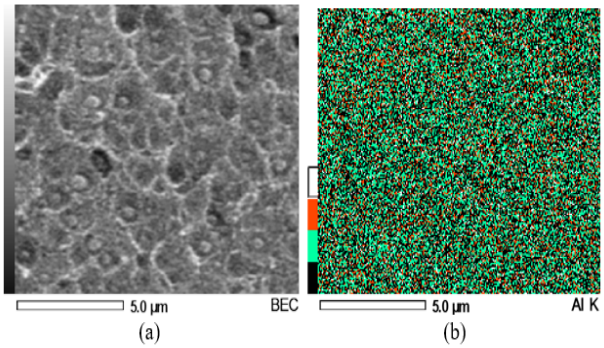

Fig. 1. SEM image (×9,500) (a) and EDX mapping of Al (b) taken on a fracture surface of sample AM10. (a) SEM image and (b) EDX mapping.

Then, let us check the spatial uniformity of the filler abundance in this sample by the above-mentioned method. Fig. 2 shows the results acquired for this sample, AM10, together with two other ones, A10 and AE10, with the filler content of 10 wt%. Here the SEM-EDX analysis was conducted at two positions on each cross-section, near the surface and around the center. Fig. 2(a) indicates that the mass% of Al, near the surface on the cross-section, increases with the increase in magnification. This increase is particularly significant in AE10. From this, the spatial filler dispersity near the surface on the cross-section of AE10 is not likely very good. The spatial filler dispersibility seems better around the center of the cross-section than near the surface in all three samples.

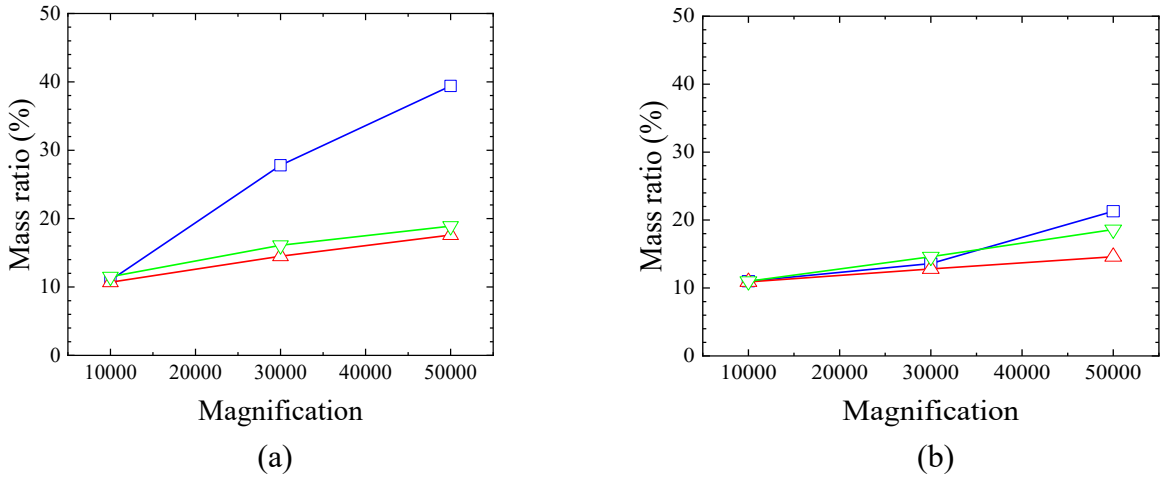

Fig. 2. Mass ratios of Al in A10 (green inverted triangles, ▽), AM10 (red upward triangles, ▲), and AE10 (blue squares, ▫), measured by SEM-EDX under different magnifications. Note that several data overlap each other. (a) near the surface and (b) around the center.

In Fig. 2, the magnification-dependent variation of the 2D mass% is the smallest in AM10, both near the surface and around the center of the cross-section, indicating the uniformity of spatial filler distribution inside the sample. In our previous paper [21], it was clarified that in polyimide NC, the adhesion between the filler and the resin is stronger and the thermal conductivity is higher in sample AM than in samples AE and A. There is a possibility that the strong filler/resin adhesion in sample AM brings about good spatial filler dispersibility inside it.

Next, let us apply the above-mentioned method to estimate the spatial dispersion of filler in samples. For

samples A10 and A20 containing boehmite alumina with no surface treatment, the observation by SEM-EDX was performed under magnifications of 10,000, 30,000, and 50,000 times at two locations on each cross-section, near the surface and around the center. Fig. 3 shows the 2D mass% of Al measured in the two samples by the EDX measurements as a function of the observation magnification.

The ratio of the mass% between samples A20 and A10, A20/A10, and its power of (3/2), namely $(A20/A10)^{3/2}$, are also shown in Fig. 3. At the two locations in both samples, the mass% of Al increases with the increase in magnification. Based on the discussion so far, the spatial filler dispersibility may not be so good. Although the 2D ratio of mass% of Al between the two samples, A20/A10, is smaller than 2.0 at all measurement points, its 3D ratio, $(A20/A10)^{3/2}$, exceeds 2.0. It is indicated that A20 contains approximately twice as much filler as A10.

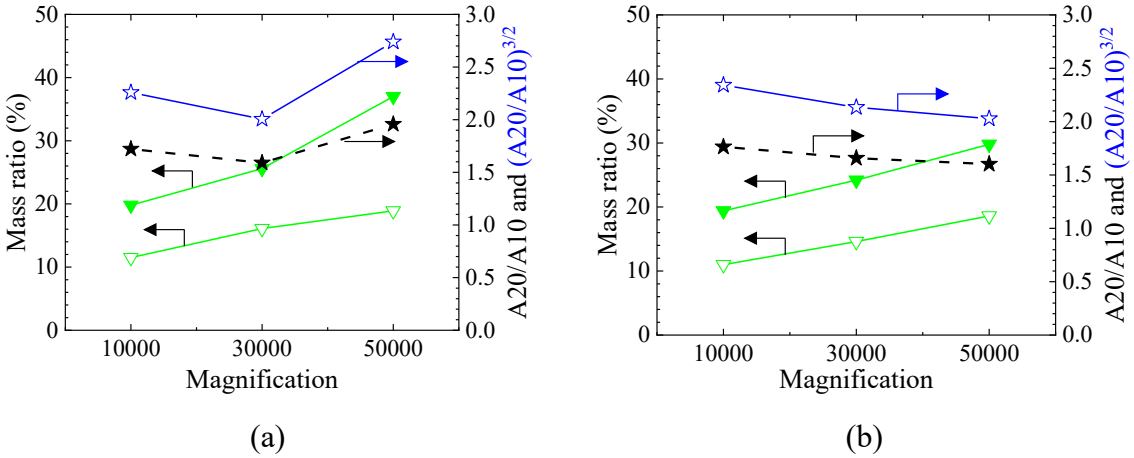

Fig. 3. Mass ratios of Al in samples A10 (▽) and A20 (▼) and their mutual ratios, A20/A10 (★) and $(A20/A10)^{3/2}$ (★), measured by SEM-EDX under different magnifications. (a) near the surface and (b) around the center.

The SEM-EDX data analyzed in this paper were not measured with the intention of evaluating the spatial filler dispersity from those data. In general, in microscopic observation, the object to be observed, such as a filler, will be captured at the center of the observation area under a low magnification at first. Then the observation magnification will be gradually increased. In this case, the atomic% or mass% of the filler to be measured would likely depend positively on the observation magnification. This would be one reason that the number of data that depends positively on the observation magnification is more than its counterpart in this paper.

Furthermore, in the case of a PNC, in which substances with significantly different resistance to electron beams are present, the observation under a high magnification or repeated SEM-EDX measurements would damage the polymer and reduce the signal intensity derived from it. The signal intensity from the inorganic substance would be enhanced accordingly.

In other words, in order to evaluate the spatial filler dispersibility from the observation magnification dependence of the atomic percentage or mass ratio of the filler as proposed in this paper, it is necessary to start the measurement at a randomly chosen place. It is also indispensable to combine the measurements conducted while increasing and decreasing the magnification. We may need to prepare a procedure manual for the evaluation.

The calculations developed in this paper are at the level of elementary mathematics. In addition, it is obvious that SEM-EDX can tell the content and distribution of fillers. Even so, as far as the authors know, there have been no papers that mentioned how to practically examine the filler content and distribution in a PNC. In the future, industrial applications of PNCs will continue to advance. In the process control in industries, we have to rely on 2D observations. Therefore, the estimation of 3D filler content and distribution in the material from the 2D observed results becomes an important issue. The authors hope that this paper will give you an opportunity to consider how to deal with this issue.

6. Conclusion

Significant contributions of Prof. Toshikatsu Tanaka to the R&D of PNCs are briefly mentioned, focusing on the mutual relation between him and the corresponding author of this paper. Several examples of industrially realized applications of PNCs in Japan are also introduced.

Equations to convert apparent 2D filler content in a PNC to the corresponding 3D value were investigated assuming cubic lattice models and a large cube model with small spherical particles. As a result, the 2D area% of the filler observed by SEM was found to be higher than the actual vol%. It was also clarified that the apparent 2D value can be approximated as the corresponding 3D value to the power of 2/3. However, for such conversion between 2D and 3D, when we calculate the abundance ratio of each constituent atom, the sum of the abundance ratios of all the constituent atoms in 3D or 2D must be 1.0.

When the atomic% or wt% is not constant when observed under different magnifications without changing the center of the observation area of SEM-EDX, the filler is not uniformly distributed in the PNC. This fact can be a method to estimate the spatial filler dispersity. However, when applying it, it is necessary to pay sufficient attention to the place where the observation is started and how to change the observation magnification. Attention should also be paid to the difference in resistance against electron beam among the composite substances.

The validity of the above two methods concerning the

filler content and distribution has been confirmed for polyimide NCs.

7. Acknowledgment

This work was partly supported by a project, Innovation Program for Energy Conservation Technologies (JPNP12004), of NEDO. The authors would like to thank N. Fujimoto and N. Hayashisaka of Sumitomo Seika Co., Ltd., T. Umemoto and H. Muto of Mitsubishi Electric Corporation, and K. Kawada of Waseda University for their help in this research.

This is an Open Access article distributed under the terms of the Creative Commons Attribution License.

References

1. Y. Ohki, IEEE Electr. Insul. Mag. **36**, 41 (2020).
2. I. Pleşa, P.V.Noţingher, C. Stancu, F. Wiesbrock and S. Schlög, Polymers, **11**, 1 (2019).
3. Y. Sun, Z. Zhang, K. Moon and C.P. Wong, J. Polym. Sci. B Polym. Phys. **42**, 3849 (2004).
4. G. Yang, J. Li, Y. Ohki, D. Wang, G. Liu, Y. Liu, and K. Tao, AIP Adv. **10**, 045015 (2020).
5. N. Tagami, Y. Ohki, T. Tanaka, T. Imai, M. Harada and M. Ochi, IEEE Trans. Dielectr. Electr. Insul. **15**, 24 (2008).
6. N. Fuse, H. Sato, Y. Ohki and T. Tanaka, IEEE Trans. Dielectr. Electr. Insul. **16**, 524 (2009).
7. H. Alamri and I.M. Low, Mater. Des. **42**, 214 (2012).
8. F.Tian and Y. Ohki, J. Phys. D Appl. Phys., **47**, 1 (2014).
9. X. Li, Y. Masuzaki, F. Tian and Y. Ohki, IEEJ Trans. Fundam. Mater. **135**, 88 (2015).
10. T. Tanaka and A.S. Vaughan, Tailoring of Nanocomposite Dielectrics—From Fundamentals to Devices and Applications, 1st ed. Pan Stanford: Singapore p. 397-413 (2017).
11. T. Tanaka and T. Imai, Advanced Nanodielectrics—Fundamentals and Applications, 1st ed.; Pan Stanford: Singapore p. 19-86 (2017).
12. Y. Ohki, IEEE Electr. Insul. Mag. **29**, 71 (2013).
13. Y. Ohki, IEEE Electr. Insul. Mag. **29**, 65 (2013).
14. Y. Ohki, IEEE Electr. Insul. Mag. **29**, 85 (2013).
15. Y. Ohki, IEEE Electr. Insul. Mag. **35**, 43 (2019).
16. Y. Ohki, IEEE Electr. Insul. Mag. **36**, 50 (2020).
17. Y. Ohki, IEEE Electr. Insul. Mag. **26**, 63 (2010).
18. https://newswitch.jp/p/28211
19. N. Hayashizaka, K. Kawasaki, M. Yamashita, T. Ebina, T. Ishida and S. Hattori, United States Patent Application Publication US20180201804A1 (2018).
20. T. Matsuzoe, N. Kita, Y. Nishigaki, T. Abe, T. Kubo, Y. Nakano, M. Kozako, M. Hikita, N. Fujimoto, N. Hayashizaka, et al., IEEE Electr. Insul. Conf. Calgary, pp. 83 (2019).
21. Y. Ohki and N. Hirai, J. Compos. Sci., **5**, 272 (2021).
22. M. Kurimoto, S. Yoshida, T. Umemoto, T. Mabuchi and H. Muto, IEEE Trans. Dielectr. Electr. Insul. **28**, 74 (2021).
23. T. Umemoto, S. Yoshida, H. Muto and M. Kurimoto, IEEE Trans. Dielectr. Electr. Insul. **28**, 282 (2021).
24. K. Tohyama, T. Iizuka, K. Tatsumi, Y. Otake, T. Umemoto, T. Mabuchi and H. Muto, IEEE Conf. Electr. Insul. Dielectr. Phenom. (CEIDP), Richland, WA, USA, pp. 78–81 (2019).
25. E. Nagase, T. Iizuka, K. Tatsumi, N. Hirai, Y. Ohki, S. Yoshida, T. Umemoto and H. Muto, IEEJ Trans. Electr. Electron. Eng., **16**, 15 (2020).
26. K. Mori, N. Hirai, Y. Ohki, Y. Otake, T. Umemoto and H. Muto, IET Nanodielectr., **2**, 92 (2019).
27. Y. Ohki, N. Hirai; T. Umemoto and H. Muto, J. Compos. Sci., **5**, 266 (2021).
28. K. Okamoto, 2020 Int. Symp. Electr. Insul. Mat. (ISEIM), Online, SP2-3 (2020). INSPEC Accession Number: 20318443.
29. N. Hayakawa, K. Kato, M. Hikita, H. Okubo, K. Watanabe, K. Adachi and K. Okamoto, IEEE Conf. Electr. Insul. Dielectr. Phenom. (CEIDP), online, 4A-3 (2020).
30. https://en.wikipedia.org/wiki/Energy-dispersive_X-ray_spectroscopy
31. M. Nentwich, T. Weigel, C. Richter, H. Stöcker, E. Mehner, S. Jachalke, D. V. Novikov, M. Zschornak and D. C. Meyer, J. Synchrotron Radiat., **28**, 158 (2021).